

RESEARCH PAPER

Structural, Optical, and Photo Detecting Properties of Radial CuO/ZnO/Si Nanostructured Heterojunction

Iman Hamza Irhayem^{1*}, Khalidah H. Al-Mayalee²

¹ University Teacher, General Directorate of Muthanna Education, Iraq

² Department of Physics, Faculty of Education for Women, University of Kufa, Kufa, Iraq

ARTICLE INFO

Article History:

Received 24 March 2025

Accepted 27 May 2025

Published 01 July 2025

Keywords:

Electrical properties

Nanostructured

Optical properties

Structural properties

ZnO/CuO heterostructure

ABSTRACT

Radial CuO/ZnO p-n heterojunctions have been successfully fabricated on Si and glass substrate. The vertically aligned ZnO nanostructures are formed at 75°C temperature using a hot water treatment technique for deposition times of (10, 20, 30) min. Using the hydrothermal method, on ZnO nanorods, high density CuO nanostructures were produced. The investigation focused on the p-n nanostructured junction's optical, structural, and morphological characteristics. The XRD results show that the constitutive layers show high crystalline quality. The FESEM images revealed a porous surface texture of the constructed CuO/ZnO heterojunction and become more densely packed at 30 min deposition times of ZnO. The results of the optical properties show that as the ZnO deposition time increases, the absorption spectra of the as-prepared CuO/ZnO moves from the UV region to the visible area. The optical energy gap values tend to decrease with increasing ZnO thin film's deposition time. The photoelectrical properties of the CuO/ZnO/Si junctions were investigated through current-voltage characteristics. Results demonstrated that the radial p-CuO-n-ZnO nanostructured junction has a good photocurrent response and recovery times due to high surface-to-volume ratio and efficient electron transport which reveal their suitability for low cost photodetector devices.

How to cite this article

Irhayem I., Al-Mayalee K. Structural, Optical, and Photo Detecting Properties of Radial CuO/ZnO/Si Nanostructured Heterojunction. J Nanostruct, 2025; 15(3):863-874. DOI: 10.22052/JNS.2025.03.005

INTRODUCTION

The importance of metal oxide nanostructured semiconductor materials was increased day by day in a wide range of applications of batteries, the packaging industry, photocatalysis, optoelectronics, sensors, and drug delivery. Metal oxide nanostructures (NSs), such as ZnO, TiO₂, and CuO, etc., were shown to have extremely advanced chemical, magnetic, optical, and biomedical properties due to their tiny particle sizes and high surface-to-volume ratio [1].

* Corresponding Author Email: imanh.almousawy@student.uokufa.edu.iq

Scientists have been very interested in zinc oxide (ZnO), a metal oxide semiconductor of the n type. due to its numerous fascinating properties, such as its electro-optical, piezoelectric, and magnetic characteristics [2-5]. ZnO nanoparticles have been extensively researched for a variety of optoelectronic, sunscreens, antimicrobial agents, and biosensing applications because to their excellent thermal stability, very wide band gap (3.37 eV), and nontoxic nature [6-8]. It is simple to create ZnO NSs at both low and high temperatures



This work is licensed under the Creative Commons Attribution 4.0 International License.

To view a copy of this license, visit <http://creativecommons.org/licenses/by/4.0/>.

[8]. CuO, also known as cupric oxide, is a p-type semiconductor that is inorganic, nontoxic, plentiful, and reasonably priced. Its bandgap ranges from 1.2 to 1.7 eV. CuO nanostructures have a considerable absorption capacity for visible light, making it a very desirable material for a variety of uses, such as pollution degradation, solar energy, batteries, sensors for gases, and catalysis [9,10,11].

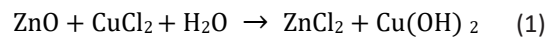
The p-n radial heterostructures of CuO and ZnO oxides of metals have garnered a lot of interest in a range of optoelectronic applications, including light-emitting diodes (LEDs), photodetectors, solar cells, and photocatalysis [12,13,14,15]. Recently, several studies have focused on the radial heterostructure that utilize ZnO nanorods as the core and a CuO thin film layer as the shell for optoelectronic devices [16,17,18]. The CuO/ZnO p-n nanostructured heterojunctions offer advantages like high photoconductive efficiency due to their high interface surface area and increased optical absorption, leading to increased photon collection efficiency [17,18]. In this work, We present the easy and cheap synthesis of CuO/ZnO heterojunctions on Si substrates for photodetector applications.

MATERIALS AND METHODS

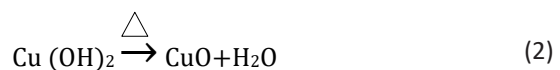
In this study, pure zinc powder with a molar mass of 65.39 g/mol and a density of 7.133 g/cm³ was used. The silicon (Si) p-type, and glass substrates were cleaned with ethanol, alcohol, and acetone each for 5 minutes to remove any residual impurities. The substrates were then washed with deionized water and dried under a stream of air. In order to synthesize ZnO nanostructures on Si and glass substrates, thin films of zinc were deposited on to the substrates using thermal evaporation method at a high vacuum pressure of (10⁻⁷ mbar). Next, the Zn/Si and Zn/glass samples

were immersed in hot deionized water at 75 °C for 10, 20, and 30 minutes to produce zinc oxide NSs. The hot water treatment (HWT) method involves immersing metallic films and substrates placed in a baker containing hot deionized water (70–100) °C. Both temperature and time are critical parameters that have an important effect on the quality of the films created. Typically, metal oxide nanostructures have been obtained by treating metals or their alloy foils in hot de-ionized water. However, only a few numbers of studies have reported on the facile treatment of metal thin films deposited on deferent bases, such as glass and Si (p-type), in hot de-ionized water to develop nanostructured metal oxide films.

The as-prepared ZnO NSs were placed in 10 mL of an aqueous solution of CuCl₂, which has a molecular weight of 170.48 gm/mol, at a concentration of 0.002M in order to form CuO/ZnO junctions. CuO/ZnO heterojunctions were formed by annealing the Cu(OH)₂/ZnO heterojunction substrates at 450 °C for an hour in air after three rounds of DI water washing. Fig. 1 shows a schematic representation of the CuO/ZnO heterojunction manufacturing. In accordance with the first equation a solution approach was used to generate Cu(OH)₂/ZnO [19].



Following annealing, the CuO/ZnO structure was obtained using the following formula.



Characterization

The field emission scanning electron

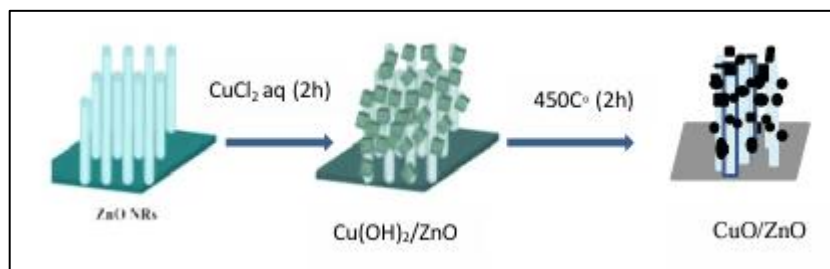


Fig. 1. A diagram showing how the CuO/ZnO hybrid junctions are synthesized.

microscope (FESEM) instrument made by MIRA3 (model TE-SCAN; Dey Petronic) with an accelerating voltage of 30 kV was used to study nanostructures morphology and size. A Thermo-scientific EDS instrument from the United States was used to determine the composition of the prepared NSs. A X-ray diffraction (XRD, Shimadzu labx XRD-6000) technique was used to determine the structure, crystal orientation, and grain size of the synthesized nanostructured films. For the optical characterizations, an ultraviolet-visible (UV-VIS) spectrophotometer (Shimadzu Model 1900i), which had wavelengths between 200 and 1000 nm, was employed. The transition energy of the materials was measured using the Perkin Elmer Spectrophotometer Luminescence LS 55, which is equipped with FL Winlab software.

RESULT AND DISCUSSION

The morphology of the resultant CuO/ZnO heterostructures is seen using FE-SEM . Fig. 2a-c confirm the conformal coverage of ZnO thin films. ZnO films were grown on silicon (Si) substrates using hot water treatment method at 75 °C for 10, 20, and 30 minutes, respectively. The FE-SEM images (a, b, c) revealed how the surface morphology of the ZnO nanostructures changes with increasing HW treatment time. However, the longer treatment times generally lead to larger and more well-defined nanostructures. CuO layers were deposited hydrothermally on top of the pre-deposited ZnO films. As shown in Fig. 2d-f, the CuO morphology was influenced by the underlying ZnO films resulting in a sea anemone-like CuO/ZnO heterostructures. This observation aligns with the

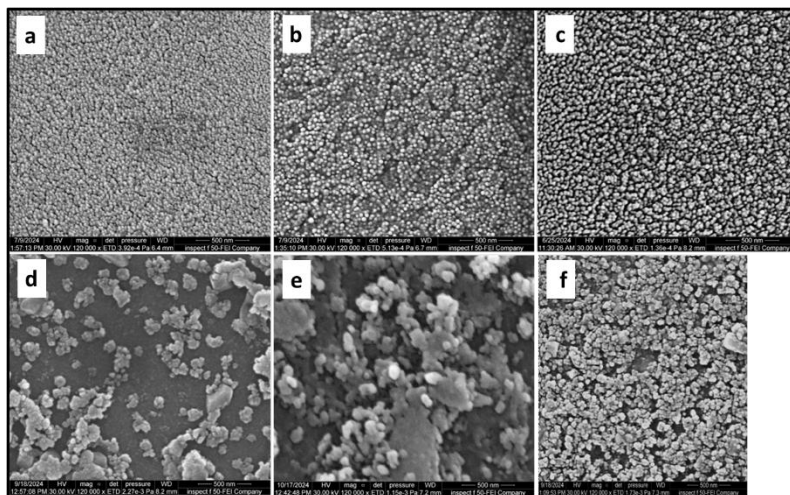


Fig. 2. FE-SEM images of ZnO nanostructured films grown on a Si substrate by HWT method at 75 °C for treatment times (a) 10 min, (b) 20 min, and (c) 30 min. Images (d), (e), and (f) are top-view FE-SEM images of CuO hydrothermally grown on the ZnO films deposited different times 10 min, 20 min, 30 min, respectively.

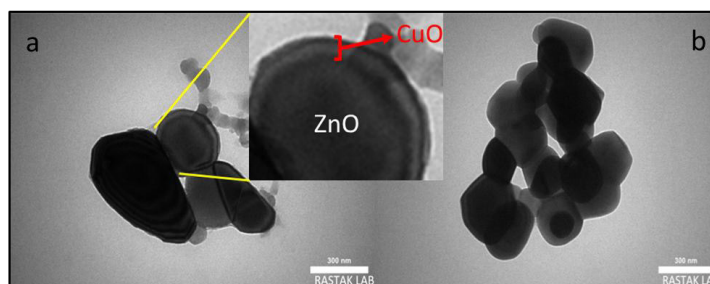


Fig. 3. pictures of the CuO/ZnO heterojunction using TEM.

results presented in [20]. ZnO thin films are clearly well covered with copper oxide. The diameters of the CuO/ZnO nanostructure grains range from 30 to 100 nm.

TEM measurements performed to the CuO/ZnO heterojunction are shown in Fig. 3. It shows a closer zone of the junction between CuO and ZnO than that of the SEM images. TEM image in in Fig. 3a demonstrate that CuO coated layer adhere to ZnO NSs robustly (particularly visible the inset).

This means that the CuO shell is strongly bonded to the ZnO core which is important for the stability and performance of the core-shell structure. The image Fig. 3b shows a cluster of these core-shell structures.

One of the created thin films' EDX images, together with the fraction of components that went into its composition, are shown in Fig. 4. It was discovered that there are no pollutants in the film, making it clean.

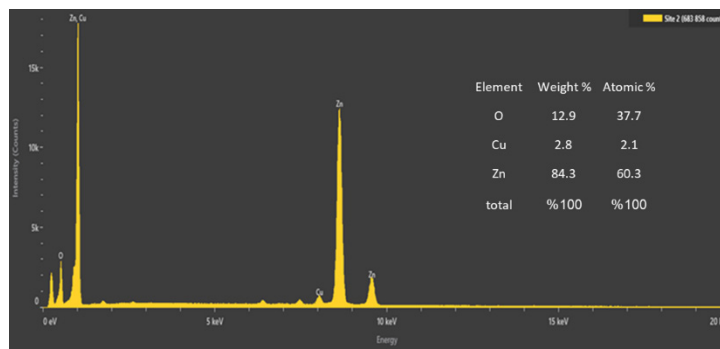


Fig. 4. EDX spectra of the CuO/ZnO film of treated Zn thin film in hot deionized water for 30 minutes, with thin film components.

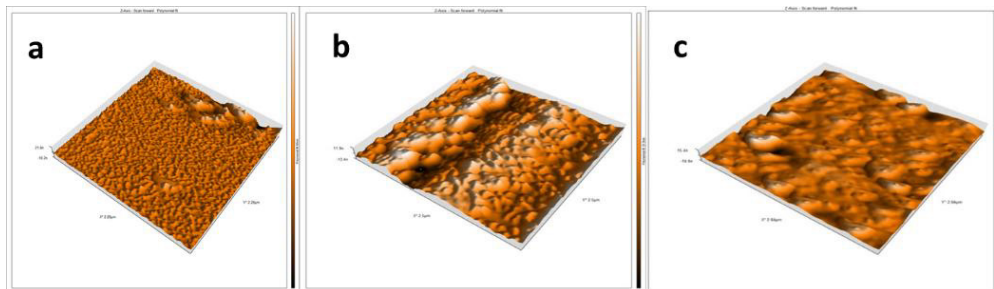


Fig. 5. 3D AFM images of the CuO/ZnO films of treated Zn thin film in hot deionized water for (a)10, (b) 20, and (c) 30 minutes.

Table 1. The root mean square (Rrms) data of CuO/ZnO/Si samples evaluated from the AFM measurements at deferent ZnO hot deionized water times (10, 20, 30) minutes.

ZnO treatment time	R _{rms} (nm)
10min	13.75
20min	24.87
30min	32.10

The surface roughness of as-synthesized CuO/ZnO films were studied at different ZnO HWT times at 75 °C using AFM (Atomic Force Microscopy). Fig. 5a-c shows the CuO/ZnO films surface morphology image as the treatment time of ZnO nanostructures increases from 10, 20 to 30 minutes respectively. The AFM images clearly show that the surface morphology of the CuO/ZnO films is greatly influenced by the duration of hot water treatment. Fig. 5a represents CuO/ZnO formation at ZnO immersing time 10 min, where small grains are nucleating and growing. After 20 min, the samples surface exhibits larger, more distinct features, and increase in surface roughness. Compared to (b), the surface in Fig. 5c appears more uniform. the estimated root mean

square (RMS) surface roughness has been of the CuO/ZnO films was listed in Table 1.

Fig. 6 displays the XRD diffraction pattern of the CuO/ZnO/Si samples for different ZnO deposition times. The generated CuO/ZnO nanostructures were confirmed using XRD peaks at 2θ positions related to the CuO/ZnO junction [8,21,22,23]. With both indices oriented to the monoclinic phase of CuO [24,25], the XRD profile in Fig. 4 shows two separate diffraction peaks at 2θ values of 35.46° and 38.78° respectively, corresponding to the lattice CuO crystal planes (002) and (111) respectively. The (002), and (110) crystal planes of ZnO are responsible for the XRD peaks at 2θ angles of 34.9° , and 58.2° , respectively. In line with earlier research, our findings also show that the ZnO

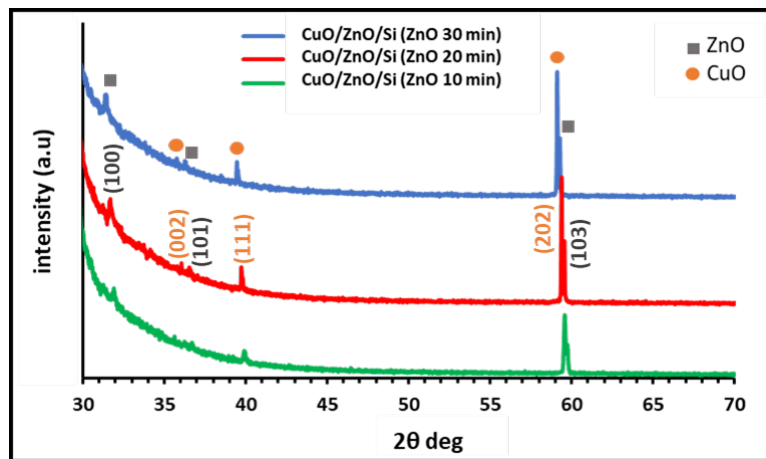


Fig. 6. XRD pattern of the nanostructured CuO/ZnO/si heterojunction

Table 2. displays structural features of the prepared films of CuO/ ZnO at the highest intensity peaks.

ZnO time	2θ deg	d (nm)	FWHM(β) rad	(D) nm	(δ) $\times 10^{-3} \text{ nm}^{-2}$
	58.5	0.158	0.003	52.9	0.36
10min	38.9	0.233	0.0048	30.40	1.08
	58.3	0.158	0.0017	93.30	0.12
20min	38.8	0.232	0.0048	30.60	1.07
	58.2	0.158	0.0016	99.12	0.10
30min	38.7	0.232	0.00478	30.73	1.06

crystal's hexagonal wurtzite phase has formed [23, 26]. Fig. 6 illustrates that ZnO nanowires have a significant XRD diffraction peak which corresponds to the ZnO (110) plane. However, the majority of ZnO nanostructures are oriented vertical to the substrate plane (Fig. 2a-c).

The XRD data was used to determine the average crystalline grain size (D) using the Debye-Scherrer equation [27]:

$$D = 0.9\lambda / \beta \cos \theta \quad (3)$$

The wavelength of an X-ray is λ , which is 0.15406 nm, β is the width in radians at half maximum, θ the diffraction angle, where K is the form factor ($K = 0.94$).

The dislocation density (δ), or the number

of lines that cut a unit area in the crystal also calculated using the grain size from the equation [28]:

$$\delta = \frac{1}{D^2} \quad (4)$$

The structural characteristics of grain size and dislocation density of the greatest intensity peaks for each of CuO at diffraction angles of 38.7° , 38.8° , and 38.9° are clearly shown in Table 2.

It can be noted from table 2 that the grain size changed as the hot deionized water time of ZnO nanostructured films increases from 10 minutes to 30 minutes. The data strongly suggests that the HWT processing is causing grain growth in the ZnO material. This means that the longer times at a 75°C allow for more atoms to diffuse and rearrange,

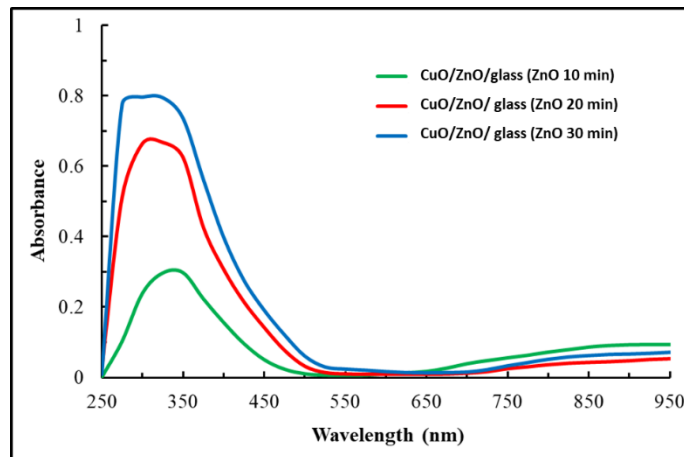


Fig. 7. The optical absorption for CuO/ZnO as a function of wavelength.

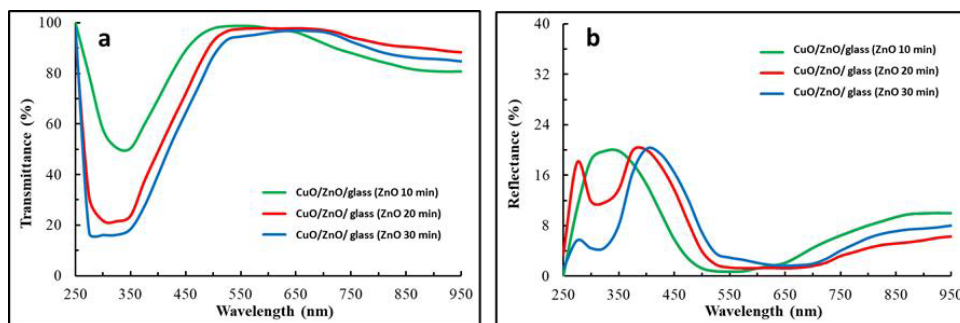


Fig. 8. (a, b). The transmittance and reflectance spectra for CuO/ZnO as a function of wavelength.

leading to larger grains. These outcomes are identical to research [27]. Also, the dislocation density (δ) decreases as time increases which indicates that the crystalline structure becomes fewer defects, more ordered, and less strained with longer deposition time.

Optical properties

The optical features were examined using the Ultraviolet-Visible (UV-VIS) spectrophotometer of the CuO/ZnO structures at wavelengths ranging from 200 to 1000 nm. Fig. 7 presented the absorbance spectra as a function of wavelength.

As illustrated in Fig. 7, the CuO/ZnO junctions for all samples absorbs light within 260–480 nm wavelength range. The results of these broad absorption peaks is consistent with previous research on CuO/ZnO nanostructured junctions [29, 30]. The observation reveals that as the hot water treatment time of ZnO increases, the amount of absorbing light by the produced CuO/ZnO interface also increases. The increasing treatment time may induce more surface defect in the ZnO films, increasing its surface area, and roughness, which enhance light trapping and increases the amount of light absorbed by CuO/

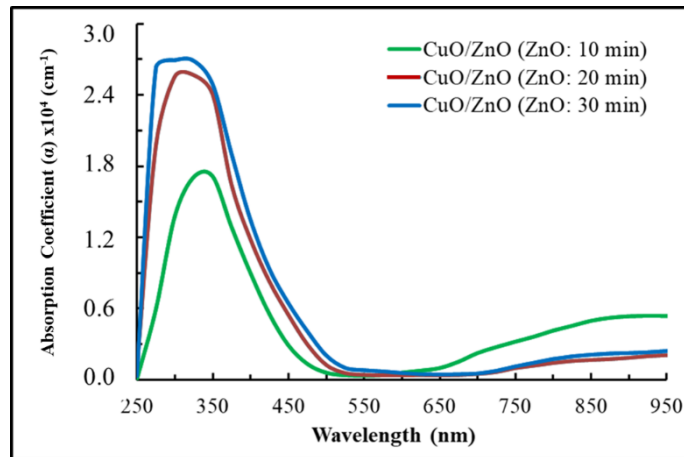


Fig. 9. Absorption coefficients of the samples with different ZnO synthesis time.

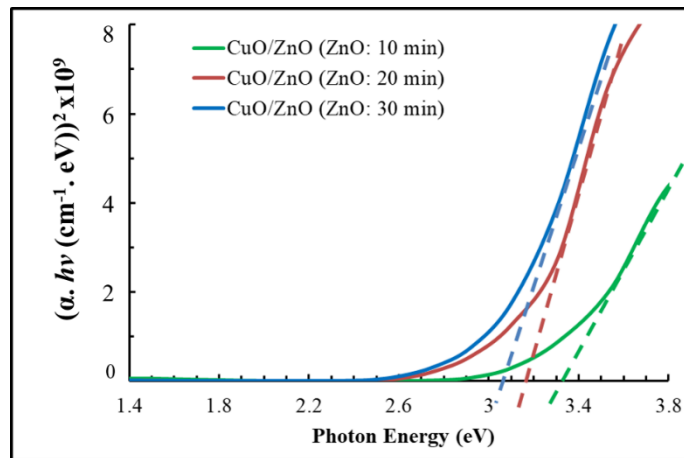


Fig. 10. Energy gap values for the CuO/ZnO hybrid junction for different ZnO preparation times.

ZnO junction [30].

Fig. 8a displays the variation in visual transmittance of the CuO/ZnO/Si structures as a function of wavelength and ZnO films deposition time (10, 20, and 30 minutes). The optical transmittance of the CuO/ZnO nanostructured interface decreased from 90% to 85% with increasing deposition time. This can be attributed to increasing ZnO thickness and surface roughness

with increasing ZnO film deposition time in a CuO shell/ZnO core structure. However, a thicker film can increase the interaction between light and material leads to more absorption and scattering of light, resulting in a decrease in transmittance through CuO/ZnO architectures [31].

Eq. 5 [32] is used to create The coefficient of absorption (α) of the CuO/ZnO directions of transition:

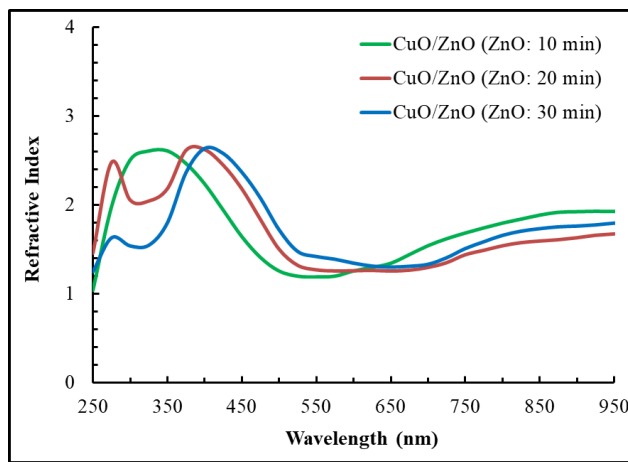


Fig. 11. Shows the refractive index as a function of the wavelength of the CuO/ZnO structures for the three different ZnO deposition times of 10, 20, and 30 min by HWT method.

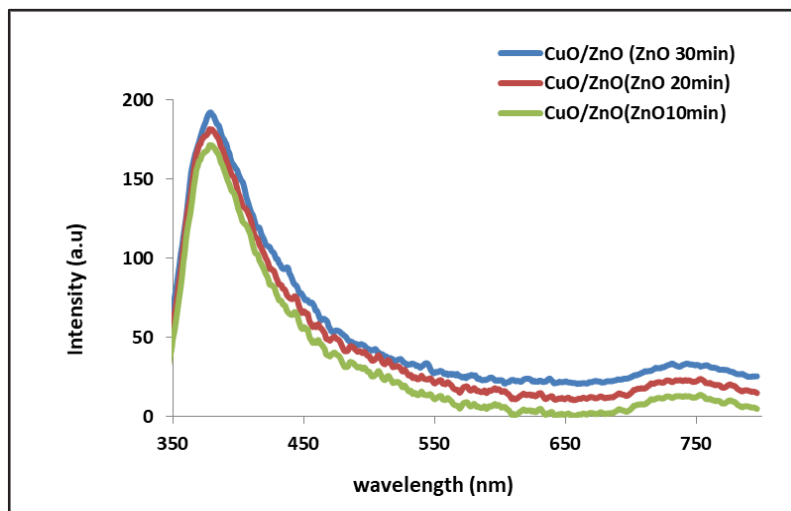


Fig. 12. The photoluminescence (PL) spectra for CuO/ZnO junctions on Si substrate with different ZnO prepared time.

$$\alpha = \frac{\ln \frac{1}{T}}{t} \tag{5}$$

Where (t) is the film's thickness, and (T) is the transmittance of the CuO/ZnO films. Fig. 9 displays absorption coefficients spectra of the CuO/ZnO samples with different ZnO synthesise time. As can be seen in Fig. 5, the maximum value of the absorption coefficient of CuO/ZnO heterojunctions are at the edge of absorption [33]. The highest absorption coefficients occur for CuO/ZnO nanostructured films. Furthermore, the absorption coefficient increases with the increasing ZnO hot water treatment time. The increased size of the crystallite might be the cause of this, it made the grain boundaries smaller. Additionally, the thickness increase may have caused more optical scattering, which would have raised the absorption coefficient's value [34].

Utilizing the absorption coefficient data, The energy gap was computed. Fig. 10 Explain α^2 vs. hu in, where α is the spectrum absorption coefficient and (hu) is the energy of the incoming photon, considering that the electron travels straight between both conduction and valence bands, equation (6) is used to calculate the energy gap (E_g) [32]:

$$\alpha h\nu = k(h\nu - E_g)^{1/2} \tag{6}$$

The CuO/ZnO hybrid junction's energy gap values shift from 3.32 eV to 3.17 eV and then to 3.05 eV, corresponding to ZnO synthesise time of (10 ,20,30) min, respectively as displayed in Fig. 10. This outcome is consistent with the previous researcher's findings [29, 30,35]. The energy gap values of the interface of the joined martials conform that the longer fabrication times might introduce more defects into the ZnO nanostructures, which can decrease the optical energy gap [34]. In addition, the varying duration of the HWT process used to form the ZnO nanostructured layer can cause strain at the interface between the CuO and ZnO, which may also affect the energy gap CuO/ZnO heterojunctions [33].

The refractive index was computed using the next relation [36]:

$$n = \frac{1+\sqrt{R}}{1-\sqrt{R}} \tag{7}$$

where n refractive index, R: Reflectivity of prepared films. It is evident from Fig. 7 that the refractive index of the CuO/ZnO junction varies with the amount of time spent preparing (ZnO). The refractive index values in our study fall between 2.5 and 2 as shown in Fig. 7, which is proportionate to the values found in previous research for the combined CuO/ZnO junction [37].

The optical photoluminescence (PL) spectra of the CuO/ZnO junctions at different ZnO NSs

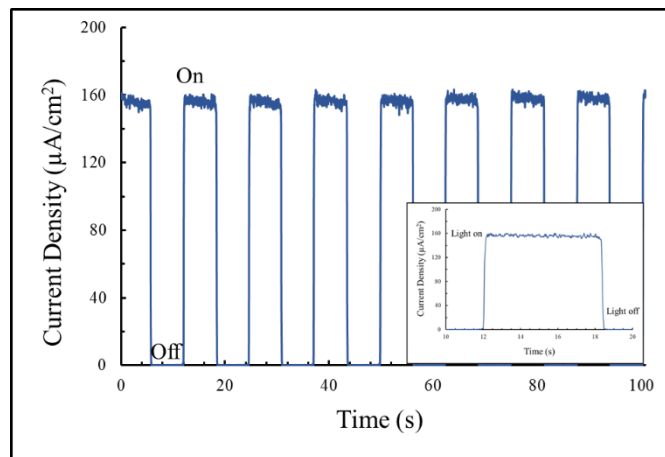


Fig. 13. The CuO/ZnO/Si devices' photocurrent response vs. time profiles under zero bias are shown in the inset, which enlarges a section of the current density vs. time.

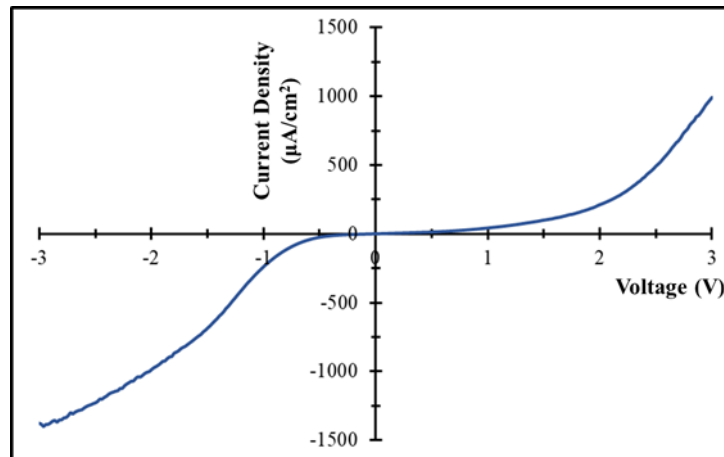


Fig. 14. Photocurrent-voltage curves (J-V) of CuO/ZnO/Si heterojunction.

synthesize times (10, 20, 30 min) are shown in Fig. 12. The excitation wavelength is 326 nm for all sample. In general, a relatively broad PL band extends from the ultraviolet (350 nm) to visible region (500 nm), associated with energy band gaps of 3.32 eV, 3.17 eV, and 3.05 eV, for the CuO/ZnO nanostructured films. This is consistent with earlier studies [35,38]. The broad PL band could be attributed to the presence of various electronic transitions within the CuO/ZnO interfaces as well as surface states [35].

Electrical properties

To study the use of the nanostructured interface between p-CuO and n-ZnO in optoelectronics, the electrical properties of ZnO/CuO film for ZnO preparation time 30 minutes were studied using I-V measurements. Fig. 13 presents the photocurrent density versus time during light-on and light-off of the ZnO/CuO/Si photoconductive devices under zero bias. The dynamic profile of the photocurrent response was studied under white lighting of (100 mW cm^{-2}), normal incidence light conditions, and the light on/off cycle was 100 seconds.

As we can see from Fig. 13, the photocurrent response exhibited relatively stable and good reproducibility throughout the on-off cycle. CuO/ZnO/Si heterojunctions demonstrate an acceptable photocurrent density (J_{ph}) value of around $155 \mu\text{A/cm}^2$, making this simple photoconductive device candidate for a low-cost photodetector device. The reasons behind the photocurrent enhancement of CuO/ZnO/Si structures at a ZnO treatment time of 30 minutes is due to the large surface area

of the CuO/ZnO nanostructured contact, which facilitates enhanced light absorption by increasing the optical path length [39,40]. Additionally, the radial heterojunction between the CuO/ZnO p-n interface allows for easy charge carrier to transfer through the junction and improve the carriers collection efficiency [40,41].

The I-V characteristic curve of CuO/ZnO/Si heterostructures with a 30-minute ZnO synthesize time is presented in Fig. 14. It is observed that nanostructure has a rectifying behaviour. Fig. 14 reveals that under a forward bias (when a positive voltage is applied to the CuO shell layer), the photocurrent increased while under reverse bias the CuO/ZnO p-n restricts current flow, and photocurrent density was quite low. The reason for this behaviour is attributed to the fact that the p-n heterojunction under a reverse bias, the resistance of the CuO/ZnO p-n junction is higher than under a forward bias voltage. These results make the nanostructured diode-like CuO/ZnO potentially useful for optoelectronic devices such as solar cells, photodetectors, and LEDs.

CONCLUSION

P-CuO/n-ZnO heterojunctions were produced on the silicon and glass substrates via the hydrothermal technique. ZnO nanorod arrays were formed on the si and glass substrates using the facial hot deionized water treatment method for varying immersing time (10, 20, 30 min). The experiment results explore the controlled growth of ZnO nanostructures and combined CuO layer to form ZnO/CuO heterostructures. FESEM

indicated that the produced CuO/ZnO films have a sea anemone morphology with high surface area. The TEM image revealed the successful formation of CuO shell/ZnO core nanostructured heterojunctions. EDX showed purity and absence of contaminants of the thin films. XRD analysis estimated the crystal sizes to be vary from 30 to 99 nanometers. According to the UV-VIS analysis, the optical absorption of ZnO/CuO films were 48%, 52%, and 63% for CuO/ZnO junctions at ZnO deposition time 10, 20, and 30 min, respectively. Additionally, the optical transmittance values decreased with increasing ZnO treatment times. The results exhibit that the produced hybrid junction's energy gap varies from (3.32-3.05) eV as the ZnO deposition duration increased. Our analysis of the produced samples' refractive indices revealed that they vary between 2.5 and 1.8 based on variations in the ZnO films' deposition times. The I-V curve shows that the CuO/ZnO junction exhibits rectifying behavior. We believe that the fabricated CuO/ZnO/Si heterostructures with promising characteristics could lead to development of improved optoelectronic devices.

CONFLICT OF INTEREST

The authors declare that there is no conflict of interests regarding the publication of this manuscript.

REFERENCES

- Zhang Q, Liu S-J, Yu S-H. Recent advances in oriented attachment growth and synthesis of functional materials: concept, evidence, mechanism, and future. *J Mater Chem.* 2009;19(2):191-207.
- Mahdi MA, Khadayeir AA, Dahash IB, Shaheed MA. Structural properties of Zn doped CuO thin film by DC magnetron sputtered. *AIP Conference Proceedings: AIP Publishing;* 2023. p. 070033.
- Ando K, Saito H, Jin Z, Fukumura T, Kawasaki M, Matsumoto Y, et al. Magneto-optical properties of ZnO-based diluted magnetic semiconductors. *J Appl Phys.* 2001;89(11):7284-7286.
- Sharma P, Gupta A, Rao KV, Owens FJ, Sharma R, Ahuja R, et al. Ferromagnetism above room temperature in bulk and transparent thin films of Mn-doped ZnO. *Nature Materials.* 2003;2(10):673-677.
- Kumar BR, Rao TS. Structural and optical properties of DC reactive magnetron sputtered zinc aluminum oxide thin films. *AIP Conference Proceedings: AIP Publishing LLC;* 2014. p. 118-122.
- Ghosh R, Fujihara S, Basak D. Studies of the optoelectronic properties of ZnO thin films. *J Electron Mater.* 2006;35(9):1728-1733.
- Park JY, Song DE, Kim SS. An approach to fabricating chemical sensors based on ZnO nanorod arrays. *Nanotechnology.* 2008;19(10):105503.
- Zainelabdin A, Zaman S, Amin G, Nur O, Willander M. Optical and current transport properties of CuO/ZnO nanocoral p-n heterostructure hydrothermally synthesized at low temperature. *Appl Phys A.* 2012;108(4):921-928.
- Siavash Moakhar R, Hosseini-Hosseinabad SM, Masudy-Panah S, Seza A, Jalali M, Fallah-Arani H, et al. Photoelectrochemical Water-Splitting Using CuO-Based Electrodes for Hydrogen Production: A Review. *Advanced materials (Deerfield Beach, Fla).* 2021;33(33):e2007285-e2007285.
- Zhu YW, Yu T, Cheong FC, Xu XJ, Lim CT, Tan VBC, et al. Large-scale synthesis and field emission properties of vertically oriented CuO nanowire films. *Nanotechnology.* 2004;16(1):88-92.
- Cao M, Hu C, Wang Y, Guo Y, Guo C, Wang E. A controllable synthetic route to Cu, Cu₂O, and CuO nanotubes and nanorods. *Electronic supplementary information (ESI) available: EDS patterns of nanotubes and SEM images of nanorods. Chem Commun.* 2003(15):1884.
- Oneizah LHA, Kareem QS, Shaheed MA. Investigation of the non-linear optical characteristics of gold nanoparticles doped with distilled water (DDDW) by laser. *AIP Conference Proceedings: AIP Publishing;* 2025. p. 040022.
- Choi JD, Choi GM. Electrical and CO gas sensing properties of layered ZnO-CuO sensor. *Sensors Actuators B: Chem.* 2000;69(1-2):120-126.
- Ghosh A, Show BB, Ghosh S, Mukherjee N, Bhattacharya G, Datta SK, et al. Electrochemical synthesis of p-CuO thin films and development of a p-CuO/n-ZnO heterojunction and its application as a selective gas sensor. *RSC Adv.* 2014;4(93):51569-51575.
- Hussain SA, Radi AJ, Najim FA, Shaheed MA. Structural, Optical and Sensing Properties of ZnO:Cu Films Prepared by Pulsed Laser Deposition. *Journal of Physics: Conference Series.* 2020;1591(1):012088.
- Zhu Y, Sow CH, Yu T, Zhao Q, Li P, Shen Z, et al. Co-synthesis of ZnO-CuO Nanostructures by Directly Heating Brass in Air. *Adv Funct Mater.* 2006;16(18):2415-2422.
- Jung S, Jeon S, Yong K. Fabrication and characterization of flower-like CuO-ZnO heterostructure nanowire arrays by photochemical deposition. *Nanotechnology.* 2010;22(1):015606.
- Guo Z, Chen X, Li J, Liu J-H, Huang X-J. ZnO/CuO Hetero-Hierarchical Nanotrees Array: Hydrothermal Preparation and Self-Cleaning Properties. *Langmuir.* 2011;27(10):6193-6200.
- Soejima T, Takada K, Ito S. Alkaline vapor oxidation synthesis and electrocatalytic activity toward glucose oxidation of CuO/ZnO composite nanoarrays. *Appl Surf Sci.* 2013;277:192-200.
- Xu L, Sithambaram S, Zhang Y, Chen C-H, Jin L, Joesten R, et al. Novel Urchin-like CuO Synthesized by a Facile Reflux Method with Efficient Olefin Epoxidation Catalytic Performance. *Chem Mater.* 2009;21(7):1253-1259.
- López R, Villa-Sánchez G, Vivaldo de la Cruz I, Encarnación-Gómez C, Castrejón-Sánchez VH, Coyopol A, et al. Cupric oxide (CuO)/zinc oxide (ZnO) heterojunction diode with low turn-on voltage. *Results in Physics.* 2021;22:103891.
- Ch A, Rao KV, Chakra Ch S. Synthesis and characterization of ZnO/CuO nanocomposite for humidity sensor application. *Advanced Materials Proceedings.* 2021;1(1):60-64.
- Fang J, Xuan Y. Investigation of optical absorption and photothermal conversion characteristics of binary CuO/ZnO

- nanofluids. *RSC Advances*. 2017;7(88):56023-56033.
24. Al-Mayalee KH, Saadi N, Badrdeen E, Watanabe F, Karabacak T. Optical and Photoconductive Response of CuO Nanostructures Grown by a Simple Hot-Water Treatment Method. *The Journal of Physical Chemistry C*. 2018;122(41):23312-23320.
 25. Cheng S-L, Chen M-F. Fabrication, characterization, and kinetic study of vertical single-crystalline CuO nanowires on Si substrates. *Nanoscale research letters*. 2012;7(1):119-119.
 26. Al Abdullah K, Awad S, Zaraket J, Salame C. Synthesis of ZnO Nanopowders By Using Sol-Gel and Studying Their Structural and Electrical Properties at Different Temperature. *Energy Procedia*. 2017;119:565-570.
 27. Mubarak TH, Hassan KH, Abbas ZMA. Using X-Ray Diffraction and Scanning Electron Microscope to Study Zinc Oxide Nanoparticles Prepared by Wet Chemical Method. *Advanced Materials Research*. 2013;685:119-122.
 28. Bowen DK, Tanner BK. *High Resolution X-Ray Diffractometry And Topography*: CRC Press; 1998 1998/02/05.
 29. Mohammed RS, Aadim KA, Ahmed KA. Synthesis of CuO/ZnO and MgO/ZnO Core/Shell Nanoparticles with Plasma Jets and Study of their Structural and Optical Properties. *Karbala International Journal of Modern Science*. 2022;8(2):88-97.
 30. Li H, Zhu L, Xia M, Jin N, Luo K, Xie Y. Synthesis and investigation of novel ZnO-CuO core-shell nanospheres. *Mater Lett*. 2016;174:99-101.
 31. Xu L, Li X, Chen Y, Xu F. Structural and optical properties of ZnO thin films prepared by sol-gel method with different thickness. *Appl Surf Sci*. 2011;257(9):4031-4037.
 32. Rajendra BV, Bhat V, Kekuda D. Optical Properties of Zinc Oxide (ZnO) Thin Films Prepared by Spray Pyrolysis Method. *Advanced Materials Research*. 2014;895:226-230.
 33. Muzakki A, Shabrany H, Saleh R. Synthesis of ZnO/CuO and TiO₂/CuO nanocomposites for light and ultrasound assisted degradation of a textile dye in aqueous solution. *AIP Conference Proceedings: Author(s)*; 2016.
 34. Amakali T, Daniel LS, Uahengo V, Dzade NY, de Leeuw NH. Structural and Optical Properties of ZnO Thin Films Prepared by Molecular Precursor and Sol-Gel Methods. *Crystals*. 2020;10(2):132.
 35. Senthil Kumar P, Selvakumar M, Ganesh Babu S, Induja S, Karuthapandian S. CuO/ZnO nanorods: An affordable efficient p-n heterojunction and morphology dependent photocatalytic activity against organic contaminants. *J Alloys Compd*. 2017;701:562-573.
 36. Hussein Kadhim A, B. Hasan N. Structural and Morphological Properties of Fe₂O₃ and TiO₂:Fe₂O₃ Thin Films Prepared by Spray Pyrolysis Technique. *Journal of Kufa-Physics*. 2019;11(1):27-34.
 37. Calvo-de la Rosa J, Locquet A, Bouscaud D, Berveiller S, Citrin DS. Optical constants of CuO and ZnO particles in the terahertz frequency range. *Ceram Int*. 2020;46(15):24110-24119.
 38. Hussain M, Ibupoto ZH, Abbassi MA, Khan A, Pozina G, Nur O, et al. Synthesis of CuO/ZnO Composite Nanostructures, Their Optical Characterization and Valence Band Offset Determination by X-Ray Photoelectron Spectroscopy. *Journal of Nanoelectronics and Optoelectronics*. 2014;9(3):348-356.
 39. Zhao X, Wang P, Li B. CuO/ZnO core/shell heterostructure nanowire arrays: synthesis, optical property, and energy application. *Chem Commun*. 2010;46(36):6768.
 40. Al-Mayalee KH, Hassan LB, Karabacak T. Photocurrent Response of CuO-Shell/ZnO-Core Nanostructures Fabricated by a Hot Water Treatment Method. *SSRN Electronic Journal*. 2022.
 41. Costas A, Florica C, Preda N, Kuncser A, Enculescu I. Photodetecting properties of single CuO-ZnO core-shell nanowires with p-n radial heterojunction. *Sci Rep*. 2020;10(1):18690-18690.